Journal of Information Systems Engineering and Management
2025, 10 (29s)
e-ISSN: 2468-4376
https://jisem-journal.com/

Research Article

A fuzzy MPPT Based Solar Plant with Triple Active Full Bridge Integration to Two Grid Networks Including EV Charging Stations

Kamalakar P[1], B. Suresh Kumar[2], J. Upendar[3]

[1] Research Scholar, Electrical Engineering Department, University College of Engineering, Osmania University, Hyderabad, India
kamalakarpothulapally@gmail.com

[2]Associate Professor, Electrical and Electronics Engineering Department, CBIT (A), Hyderabad, India

[3]Assistant Professor, Electrical Engineering Department, University College of Engineering, Osmania University, Hyderabad, India

ARTICLE INFO

Received: 24 Dec 2024

Revised: 23 Feb 2025

Accepted: 28 Feb 2025

ABSTRACT

In this paper a TAFB topology connected to a solar plant for power sharing to two grid networks is introduced. One port of the TAFB is connected to solar plant which is considered to be input port with only unidirectional power flow. The other two ports are connected to two different grid networks through individual VSCs controlled by SRF controller. Each grid network is integrated with a charging station which charges the EV batteries using high rated power electronic circuits. The TAFB circuit is controlled using PSPM technique which creates phase delay in the high frequency pulse of the port bridge for transfer of power to the port.For maximum power extraction from the solar plant FIS-MPPT technique is integrated to the PSPM control. The system is operated in different operating modes varying the transfer of power between the ports by changing the phase delay of the high frequency pulse. The complete power exchange analysis is carried out using Simulink tools in MATLAB software. The modeling of modules in done using blocks from 'Specialized Powersystems' of the 'Electrical' subset in Simulink library browser. All the results are presented in graphical plotting with time as reference including measurements of voltages, currents and powers of each module.

Keywords: TAFB (Triple Active Full Bridge), VSC (Voltage Source Converter), SRF (Synchronous Reference Frame), EV (Electric Vehicle), PSPM (Phase Shift Pulse Modulation), FIS-MPPT (Fuzzy Inference System - Maximum Power Point Tracking), PSPM (Phase Shift Pulse Modulation), Simulink, MATLAB (Matrix Laboratory).

1. INTRODUCTION

For replacing the conventional ways of electrical power generation using fossil fuels renewable source electrical power generation is adopted. The power from the renewable sources is generated with natural sources likes winds, solar insolation, bio-gas, tidal waves, hydrogen-oxygen gases etc. Utilizing these natural sources efficiently is a major hurdle that today's technology is facing [1]. As the renewable power generation technology involves many converting and stabilizing components the efficiency drops to very low value. The power utilization capability from the natural sources also needs to be improved with advanced techniques and materials [2] [3]. From the mentioned renewable sources, solar insolation utilizing power generation plants are considered to be very much flexible and easy for installation.

The solar plants include multiple PV (Photo Voltaic) panels arranged in arrays placed in parallel and series combinations [4]. These array of PV panels convert solar insolation to electrical power using silicon dopped semi-conductor material. The power generation from the PV panels generates DC voltage at the output terminals. This DC voltage need to be converted to either 1-ph or 3-ph AC voltage for utilization by the loads. In conventional methods, for DC voltage stabilization and conversion of the PV power use 'conventional DC-DC boost converter' and '6-switch VSC'.

The 'conventional DC-DC boost converter' has very high output voltage ripple, high switching losses and lower efficiency when operated for higher power rating applications. Along with these drawbacks the voltage gain is also very less in the range of 2-2.5 times of the input voltage [5]. Therefore, the 'conventional DC-DC boost converter' needs higher input voltage which is a difficult task for PV panel application as the voltage levels of the PV panels are very low. Due to the high voltage requirement of the 'conventional DC-DC boost converter' a greater number of PV panels need to be connected in series. This increases the failure rate during any fault or discontinue power generation from PV panels as the series string completely stops conducting. Therefore, the 'conventional DC-DC boost converter' must be replaced with high gain boost converter to avoid these issues [6]. Along with high gain, multi-port capability also makes it reliable and efficient for power sharing between multiple networks. In order to achieve these capabilities a TAFB is integrated to the proposed system with PV panels interconnected to two networks [7]. The proposed outline of the PV panels multiple grid networks connected system with TAFB sharing powers between networks is presented in figure 1.

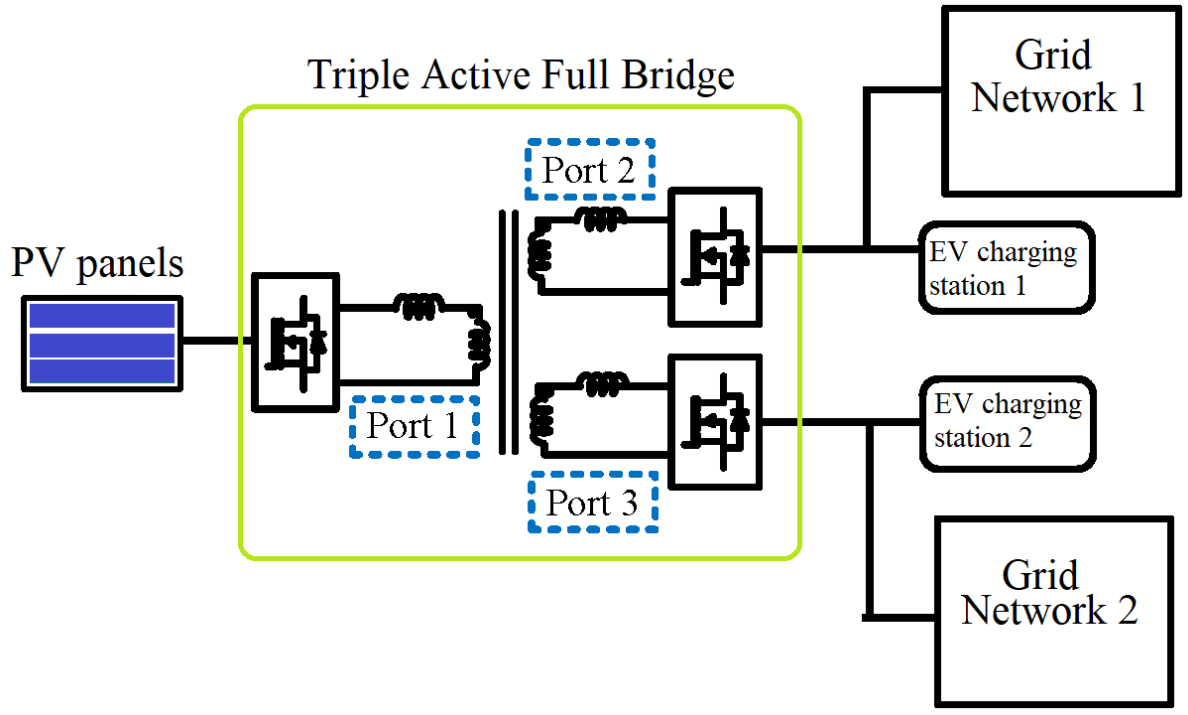

Figure 1: Structure of TAFB integrated PV panel interconnection to multiple grid networks

As per figure 1 the input port 1 is connected to PV panels and port 2 3 are connected to two individual grid networks for PV panels power sharing. Each port of the TAFB is included with four switch full bridge converter which converts the DC voltages to high frequency AC voltages [8]. All the full bridges are operated with same duty ratio however thehigh frequency pulse phases may be different which is set as per the requirement. The port 1 full bridge high frequency pulse phase will be intact as the PV panels only deliver power with no requirement of absorbing. The duty ratio of the port 1 is determined by Fuzzy MPPT for maximum power extraction from PV panels. The port 2 or 3 full bridge might vary their high frequency pulse phases with respect to requirement of power flow to the port. This phase shifting method is called PSPM technique used in most of the active full bridge topologies. The power from PV panels can be completely diverted to either of the ports and the power from port 2 or 3 can also be directed to the adjacent port using the PSPM technique. Each port 2 and 3 is also connected to individual EV charging station 1 and 2 respectively connected in parallel to the grid network [9]. The EV charging station receives power from either PV panels through TAFB or the grid network VSC.

In this paper the section 1 is included with introduction to integration of PV panel source to the multiple grid networks using TAFB structure. The outline and the techniques using in the proposed system is mentioned in this section. The following section 2 has the circuit configuration of the PV panels multiple grid networks interconnected TAFB and the Fuzzy MPPT design. The TAFB operating principle, design and control structure is explained and presented in section 3. The next section 4 has the simulation

results of the proposed system with different operating modes presenting the graphs of voltages, currents and powers of each module. The final section 5 is the conclusion to the paper finalizing and validating the graphs generated in the simulation results section followed by references.

2. SYSTEM CONFIGURATION

As previously mentioned, the proposed system comprises of four modules which include PV panels source, TAFB, EV charging station and grid networks. Each module operates at different voltage levels and powers which exchange power between each other through the TAFB circuit. Initially at port 1 the PV panels with different series and parallel string arrangement at lower voltage level are connected. The port 1 delivers power to the port 2 and 3 through the three winding HFTF (High Frequency Transformer). At the output of the port 2 and port 3 of the TAFB full bridges EV charging station and grid network are connected. The circuit structure of EV charging station and the grid network connected to the ports 2 and 3 is presented in figure 2.

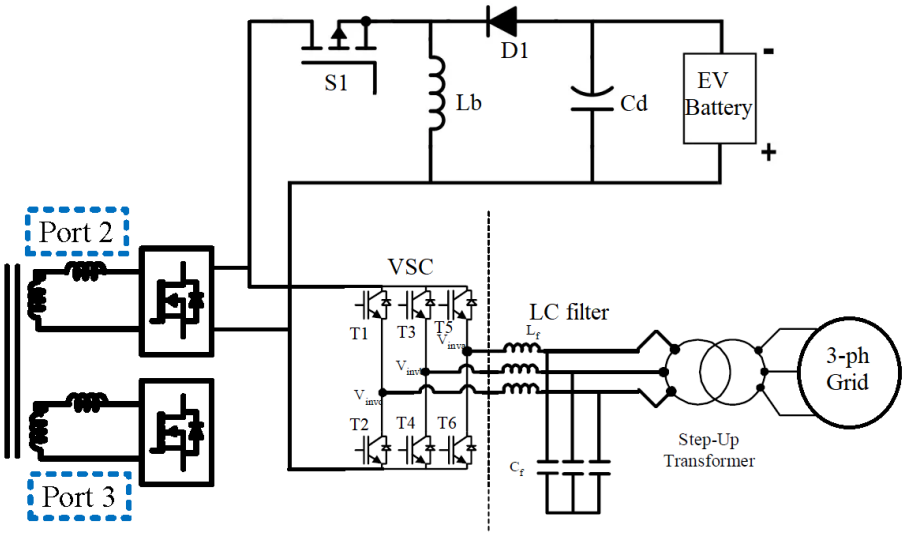

Figure 2: Circuit structure of EV charging station and the grid network

As represented in figure 2 the output of the port 2 is DC terminal which are directly connected to the 'Unidirectional Buck-Boost converter' for charging the EV battery. This 'Unidirectional Buck-Boost converter' is included with a MOSFET switch S1 which is controlled by dynamic duty ratio control [10]. Partial power from the port 2 is shared to the EV charging module for charging the battery as per the SOC (State of Charge) of the EV battery [11]. The control for the EV charging station switch S1 control is presented in figure 3.

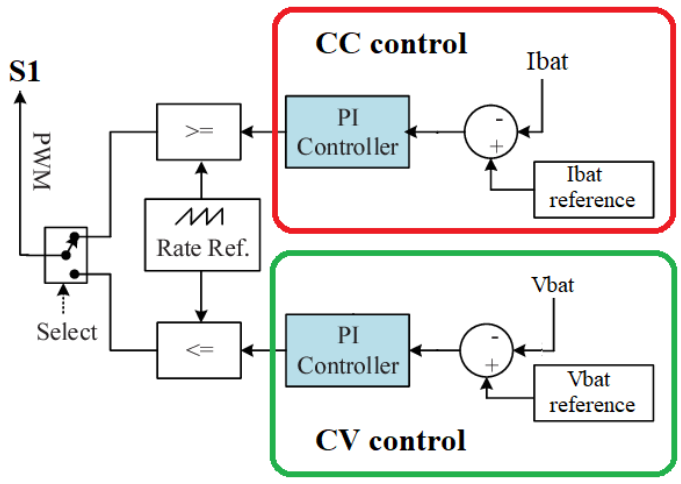

Figure 3: EV charging station control design

As represented in figure 3 the CC and CV control subsections have reference battery current and reference battery voltage values set respectively. These values are given as per the EV battery manufacturercharging capability rating. The 'CC control' mode and 'CV control' mode are selected as per the EV battery terminal voltage which varies as per the SOC of the battery pack [12]. When the SOC is above 90% the battery needs to be charged by 'CV control' mode to avoid damage to the battery with high rating charging current of 'CC control' mode [13]. The 'CC control' mode ensures high rating charging current for the battery pack for fast charging. The selection of the modes as per the voltage of the battery (Vbat) is given in figure 4.

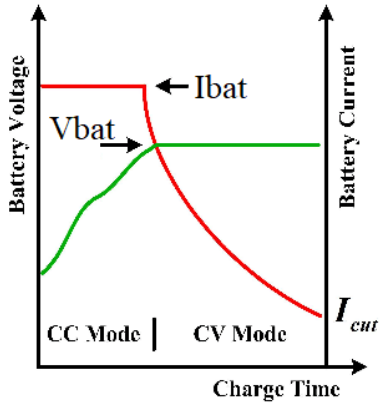

Figure 4: CC/CV mode operating currents and voltages

The 'Ibat reference' defines the maximum charge current compared to Ibat (measured) generating error current [14]. The error current defines the duty ratio of S1 with 'PI controller' current regulator. The duty ratio of the S1 is dynamically regulated for maintaining the charge current at the specified reference value. This duty ratio is compared to 'Rate Reference' carrier sawtooth waveform for generation of pulse to S1 [15] [16]. When the SOC of battery pack reaches 90% the 'CV control' is activated which defines the duty ratio as per the 'Vbat reference' value. In the 'CV control' the duty ratio of S1 is comparatively low which reduces the charging current protecting the battery cells from polarization and rupturing [17] [18].

At the DC output of the port 2 a three phase VSC is connected which interlinks the grid and the TAFB modules. The VSC operates in both rectifier or inverter modes as per the required power flow direction. The VSC comprises of 6-IGBT switches (T1-T6) which are controlled by SRF control unit with reference signals generated as per the DC voltage regulation at the output terminals of port 2. The VSC is controlled by Sinusoidal PWM (Pulse Width Modulation) technique in synchronization to the 3-ph grid source connected on the AC side of the VSC.

3. TAFB DESIGN

Each full bridge of the TAFB comprises of four MOSFETs connected in two-legged format. The MOSFETs are controlled by high frequency fixed duty ratio high frequency pulse for converting DC-AC-DC voltages [19]. The diagonal switches in the full bridge are operated simultaneously with the samehigh frequency pulse. The circuit topology with three ports of the TAFB is presented in figure 5.

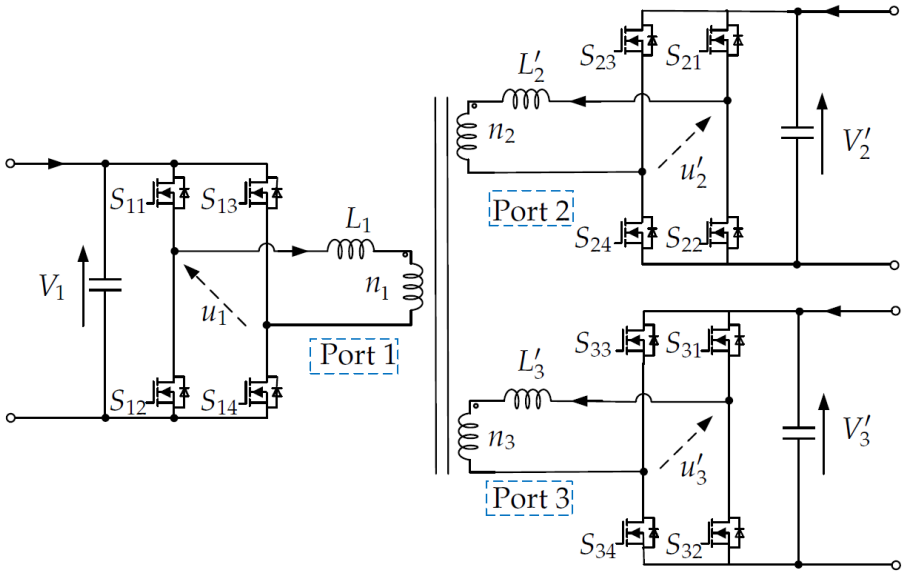

Figure 5: TAFB circuit topology

In figure 5 it is observed that the port 1 full bridge has switches ($S_{11} – S_{14}$), port 2 full bridge has switches ($S_{21} – S_{24}$) and port 3 full bridge has switches ($S_{31} – S_{34}$). All these full bridges AC sides are connected to three winding HFTF [20]. All the ports are electrically isolated and mechanically coupled through HFTF sharing powers through mutual inductance of the transformer. Each winding ratio($n_1n_2n_3$) of the HFTF can be same or different which is set as per each port voltages requirement. In the proposed system as the port 1 is connected to low voltage PV panels the windings on port 2 and 3 must be high for increased voltage development for the grid networks [21]. The high frequency pulse phase angle of the port 1 full bridge is fixed at zero as the source connected only delivers power and has no capability to absorb or store power. The other two ports 2 and 3 full bridges phase angles can be changed as per the required power exchange between the grid networks. The power possible power exchange operating modes of the TAFB is presented in figure 6.

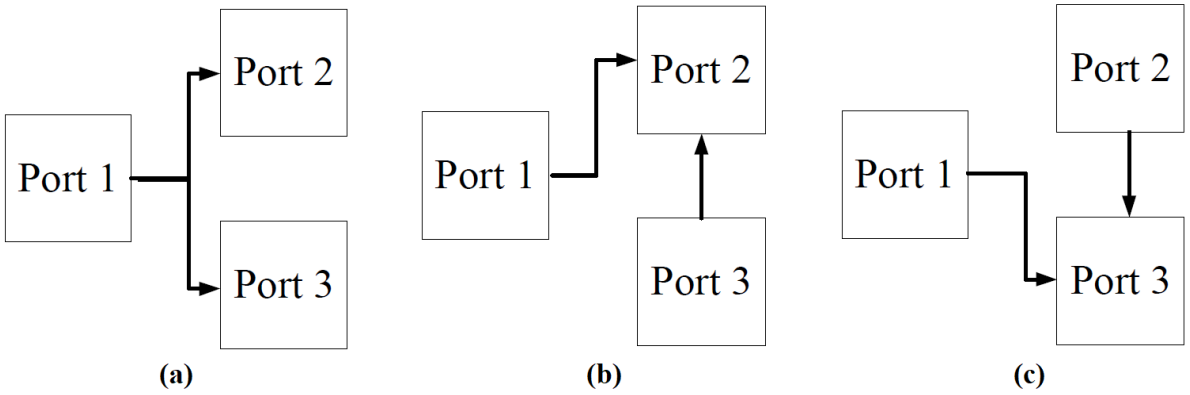

Figure 6: Operating modes (a) Port 1 to port 2 and 3 (b) Port 1 and 3 to port 2 (c) Port 1 and 2 to port 3.

The given figure 6 operating modes can be achieved by shifting the phase angle of high frequency pulse of port 2 or 3 full bridge. In first mode of operation presented in figure 6a, the phase angle of all the high frequency pulses of full bridges are maintained same sharing equal power from PV panels (port 1) to ports 2 and 3 [22]. The figure 6b operating mode is achieved by lagging phase shift created in the pulses in port 2 full bridge diverting all power from PV panels and partial power from port 3 to port 2. Similar to 6b the operating mode 6c is achieved by lagging phase shift created in the pulses in port 3 full bridge diverting all power from PV panels and partial power from port 2 to port 3 [23]. The phase shift angles of high frequency pulse of each full bridge switches for achieving different operating modes are presented in figure 7.

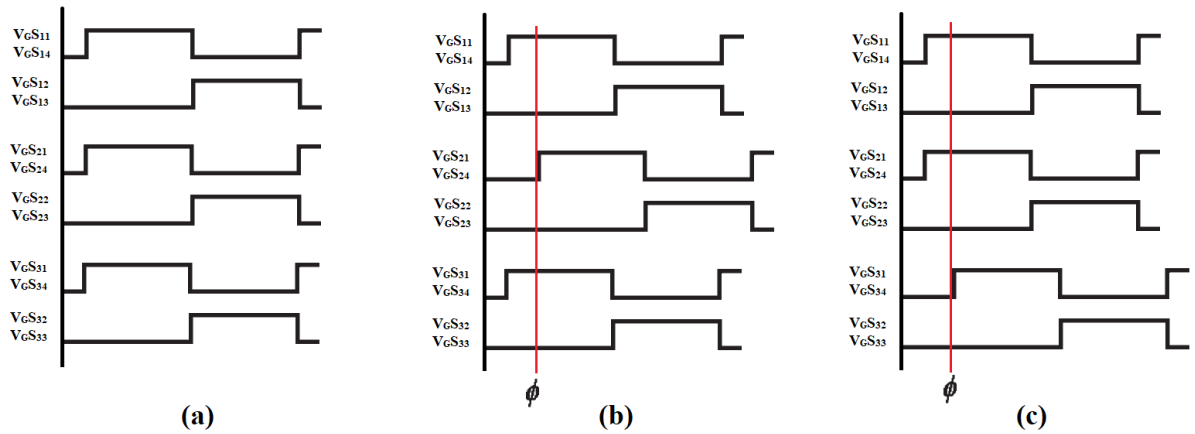

Figure 7: Phase shift of pulses of (a) Port 1 to Port 2 and 3 (b) Port 1 and 3 to port 2 (c) Port 1 and 2 to port 3

The switches S1 S4 and S2 S3 of the full bridge in all the ports operate complimentarily with fixed duty ratio of 50% [24]. The phase shift angle ϕ is created in the pulse of port 2 or 3 as per the power exchange required in the system. The power from the ports 1 2 and 3 ($P_1 P_2$ *and* P_3)with respect to phase angles of each full bridge is expressed as:

$$P_1 = \frac{V_1 V_2 \phi_2 (\pi - |\phi_2|) L_3 + V_1 V_3 \phi_3 (\pi - |\phi_3|) L_2}{2\pi^2 f (L_1 L_2 + L_2 L_3 + L_3 L_1)} \quad (1)$$

$$P_2 = \frac{V_1 V_2 (-\phi_2) (\pi - |\phi_2|) L_3 + V_2 V_3 (\phi_3 - \phi_2) (\pi - |\phi_3 - \phi_2|) L_1}{2\pi^2 f (L_1 L_2 + L_2 L_3 + L_3 L_1)} \quad (2)$$

$$P_3 = \frac{V_1 V_3 (-\phi_3) (\pi - |\phi_3|) L_2 + V_2 V_3 (\phi_2 - \phi_3) (\pi - |\phi_2 - \phi_3|) L_1}{2\pi^2 f (L_1 L_2 + L_2 L_3 + L_3 L_1)} \quad (3)$$

The ϕ_2 and ϕ_3 are the high frequency pulse phase shift angle of port 2 and 3. $L_1 L_2$ and L_3 are the filter inductances connected in series of each winding of HFTF [25]. As per the phase shift angle imposed in the pulses of the full bridge switchescreating different operating conditions are implemented. The graphs of each module measurements are presented in following section.

4. RESULT ANALYSIS AND DISCUSSION

The simulation modeling of the proposed modules of the system is designed using 'Electrical' subset blocks included in 'Specialized Technology' of the library browser in Simulink MATLAB. The TAFB HFTF is considered from 'Passives' subset with three windings selected for creating three ports in the circuit. All the blocks need to be updated with the given parameters in table 1to simulate the model and generated graphs considering different operating conditions.

Table 1: Configuration parameters

Name of the Unit	Parameter values
PV array	V_{mp} = 29.42V, I_{mp} = 7.99A, V_{oc} = 36.96V, I_{sc} = 8.48A, N_p = 9, N_s = 10, P_{pv} = 21.1kW
TAFB	P_n = 30kVA, f_n = 50kHz, n = 2, L_m = 1000µH R_p = 0.32Ω, L_p = 1µH, R_{s1} = R_{s2} = 0.64Ω, L_{s1} = L_{s2} = 2µH
EV charging station	V_{nom_bat} = 250V, Capacity = 40Ah L_{buck} = 1mH, C_o = 1000µF, R_{igbt} = 0.01Ω V_{bat_ref} = 300V, I_{bat_ref} = 20A, K_{pv} = 0.1, K_{iv} = 0.023, K_{pc} = 0.0075, K_{ic} = 0.0002.
Inverter	R_{igbt} = 1mΩ, f_c = 5kHz, V_{dcref} = 500V,

	Lf = 250µH, Cf = 10kVAR
Utility grid	Network 1 = 2500MVA 132kV, 50Hz Network 2 = 2500MVA 132kV, 50Hz

After updating the simulation model with the given parameters, the system is simulated for time of 1sec with different operating conditions set in the solar irradiation and phase delay. Initially the solar irradiation is set with constant value of 1000W/m² throughout the simulation with no phase delay in the pulses of the port full bridges. As there is no phase delay the maximum power extracted from the PV panels is shared to the two networks equally. The graphs of the voltage, current and power measurements of all the modules are presented in the figures below.

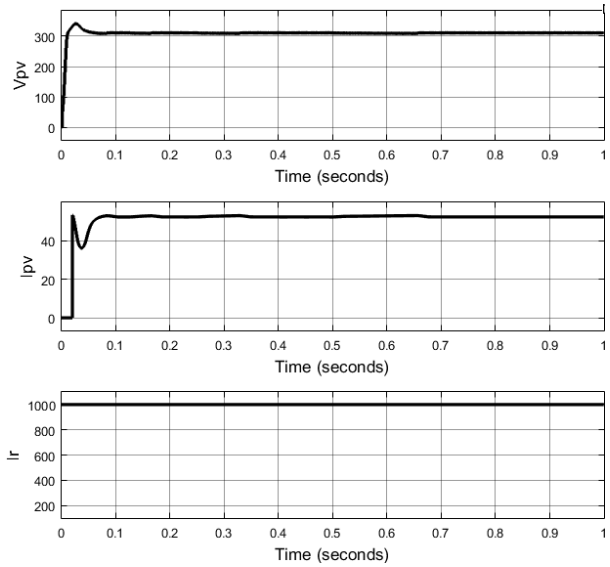

Figure 8: PV source characteristics for constant irradiation of 1000W/m²

The figure 8 includes the characteristics of PV source when operated with constant solar irradiation of 1000W/m². It can be seen that the voltage and current of the PV panels is constant throughout the simulation. The complete power from the PV panels is maximum extracted by the Fuzzy MPPT technique and delivered to the HFTF through port 1 full bridge.

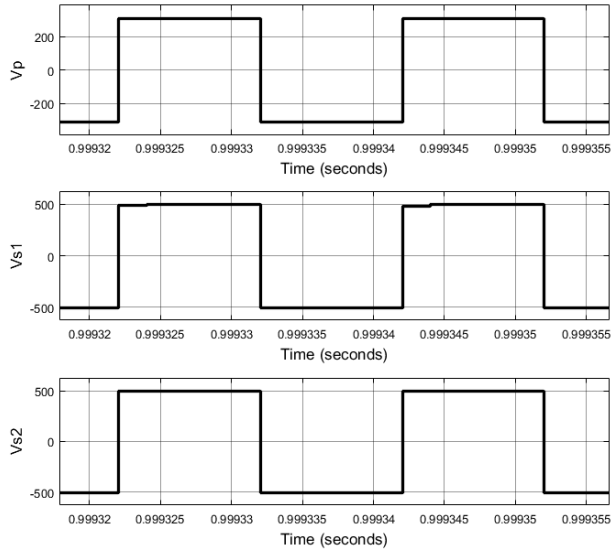

Figure 9: HFTF winding voltage with no phase delay

The primary and secondary voltages of the three winding HFTF with no phase delay is presented in figure 9. The voltages are high frequency square waveforms generated by the full bridges. As observed

the primary winding voltage magnitude is 250V and secondary windings voltages are 500V which is double due to twice winding ratio on the secondary side.

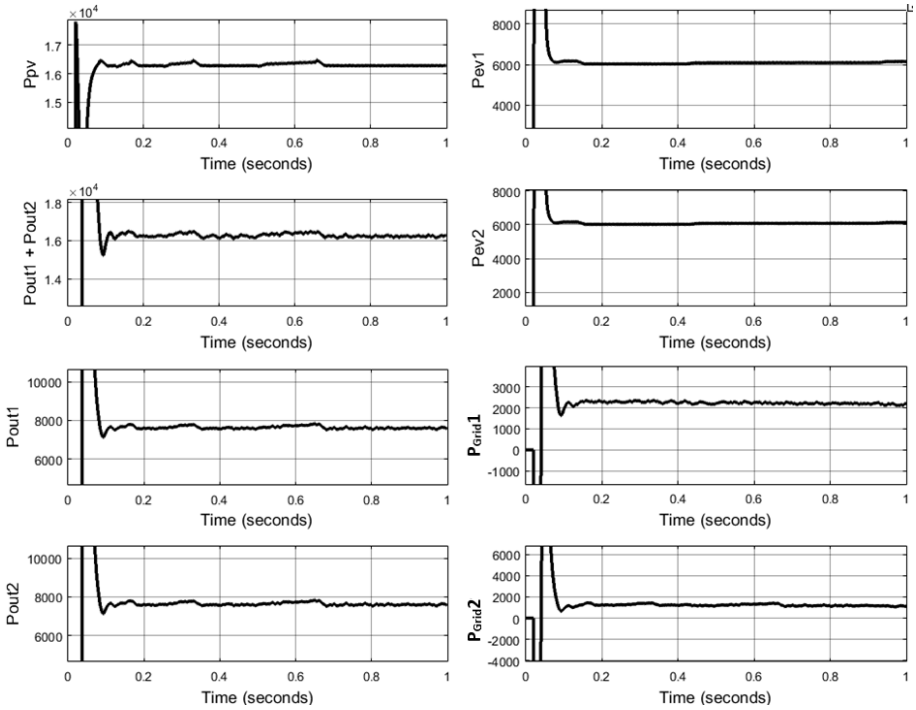

Figure 10: Active powers of all modules for constant solar irradiation and no phase delay

The active powers of all the modules in the proposed system with constant solar irradiation and no phase delay condition is presented in figure 10. The total power extracted from PV panels is 16.2kW which is equally split to 8kW and injected to the port 2 and 3 (Pout1 and Pout2) respectively. From the 8kW of PV panels power 6kW is consumed by the EV charging station of each network (Pev1 and Pev2). The remaining power of 2kW in each port 2 and 3 is delivered to the grid through the VSC connected between the full bridge and the grid.

In the next operating condition, the solar irradiation is varied at different time instants of the 1sec simulation time. However, the 'no phase delay' is maintained in the full bridge pulses of the TAFB. Initially at 0sec the solar irradiation is set to 1000W/m² which is changed to 500700W/m², 200W/m² and 800W/m² at 0.2sec, 0.4sec, 0.6sec and 0.8sec of simulation time respectively. For the given solar irradiation conditions the figure 11 represents the PV panels characteristics.

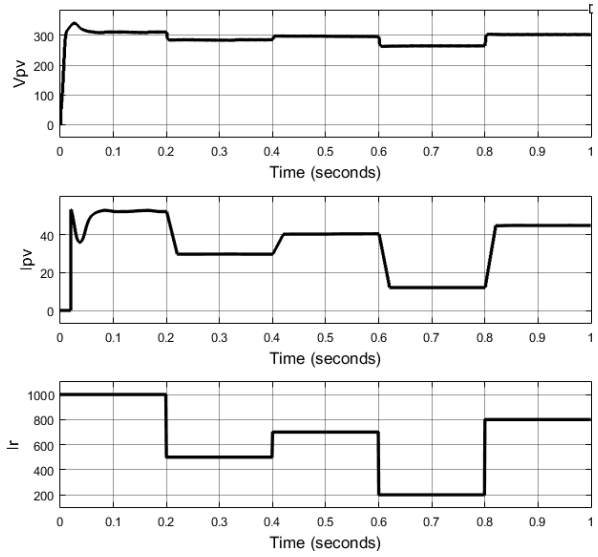

Figure 11: PV source characteristics with variable solar irradiation

As presented in figure 11 the PV panels voltage remains almost stable at 300V with negligible fluctuations but the current magnitude varies linearly as per the solar irradiation. As per the current change in the PV panels the power generated by the panels also changes. The PV panels power changes from 16kW to 8kW, 8kW to 12kW, 12kW to 4kW and 4kW to 14kW at 0.2sec, 0.4sec, 0.6sec and 0.8sec simulation time respectively. All active powers of the modules for the 'variable solar irradiation' and 'no phase delay' in full bridges is presented in figure 12.

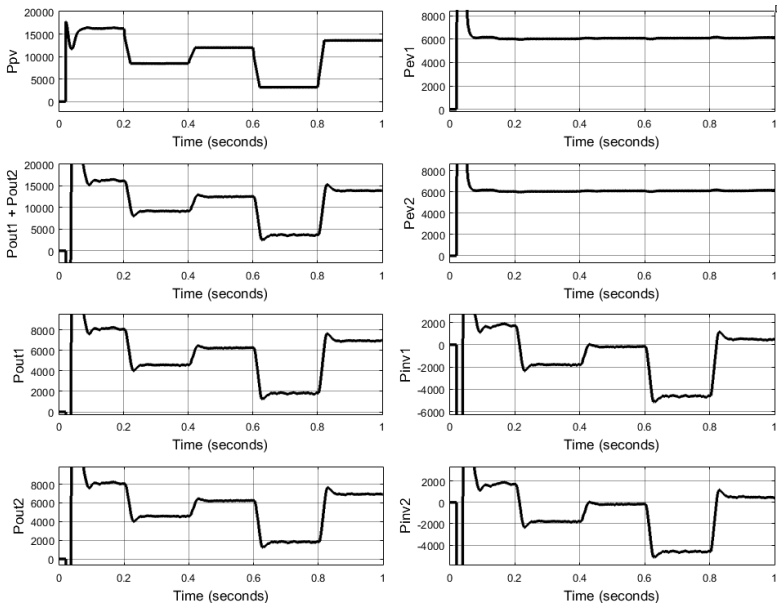

Figure 12: Active powers of all modules for variable solar irradiation and no phase delay

As per the change in PV panels powers the power delivered to the port 1 and 2 is also changed with half split power delivered to the ports. The power delivered to each port (2 or 3) changes from 8kW to 4kW, 4kW to 6kW, 6kW to 2kW and 2kW to 7kW at 0.2sec, 0.4sec, 0.6sec and 0.8sec simulation time. In any given solar irradiation condition each EV charging station consumes power of 6kW which is either compensated completely by PV panels or the grid (during lower PV panels power condition).

In the next operating condition, the solar irradiation is maintained at 1000W/m²and a lagging phase delay is created on port 2 full bridge for power transfer from port 1 and 3 to port 2. The figure 13 represents the winding voltages of the HFTF with phase delay in the port 2 winding.

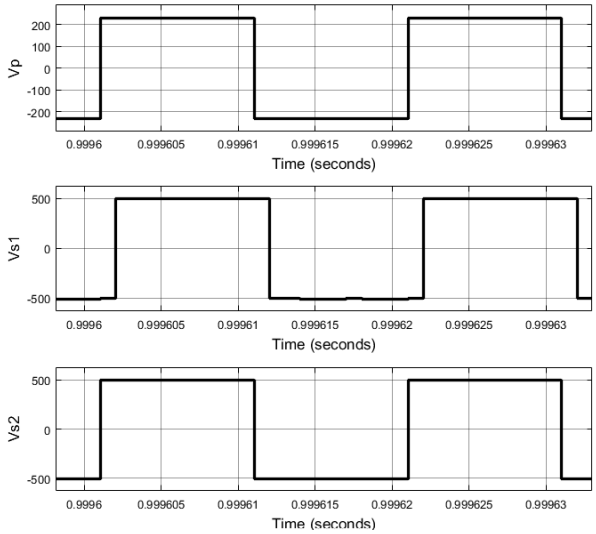

Figure 13: HFTF winding voltage with phase delay in port 2

As per the given constant solar irradiation and phase delay in port 2 the active powers of all the modules are presented in figure 14. The PV panels power delivered is 14kW which is completely delivered to port

2. Along with PV panels power from port 1, the power from port 3 of 43kW is also delivered to port 2 due to the phase delay caused in port 2 full bridge. A total power of 50kW from PV panels and port 3 grid network is delivered to port 2 grid network. From the combined power of 14kW and 43kW which is 57kW, there is a power loss of 7kW during the conversion between the TAFB and VSCs.

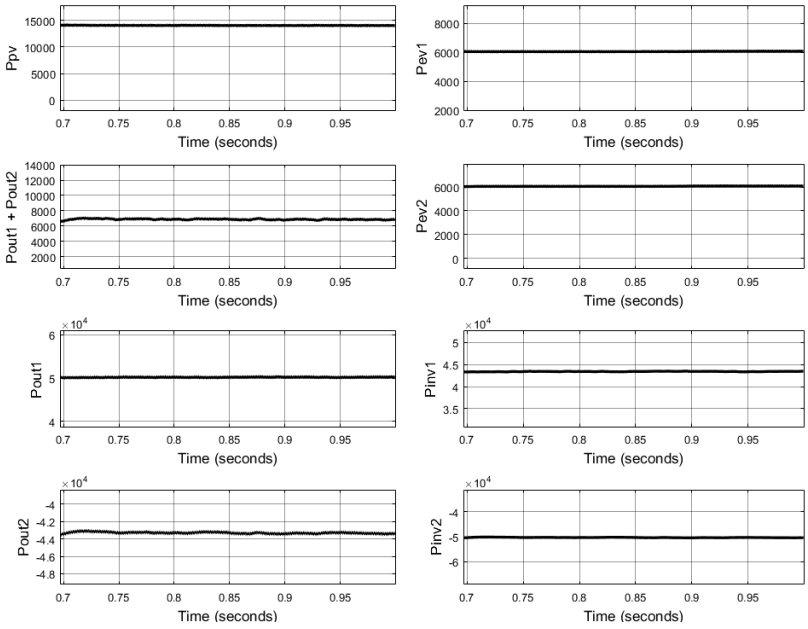

Figure 14: Active powers of all modules for constant solar irradiation and phase delay in port 2

Irrespective of the power exchange between the ports, the power consumed by the EV charging stations is 6kW individually. The power to the EV charging stations is compensated either by the PV panels or the grid networks as per the availability.

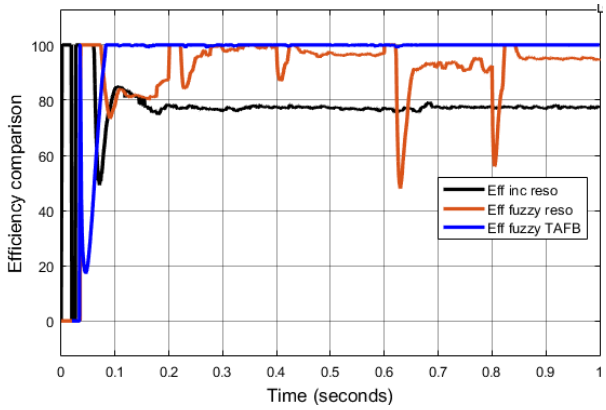

Figure 15: Efficiency comparison with different MPPTs and converters

An efficiency comparison graph is presented in figure 15, including resonant converter operated with Incremental conductance MPPT, resonant converter operated with Fuzzy MPPT and TAFB operated with Fuzzy MPPT. As per the comparison it is clear that the efficiency of the TAFB is near to 100% as compared to conventional resonant full bridge converter operating with any MPPT technique.

5. CONCLUSION

The system with PV panels connected to two individual grid networks with power sharing through TAFB topology is modeled and simulated. The proposed test system is operated in different operating conditions to validate the performance of the TAFB circuit topology. It is determined that in any given solar irradiation condition with no phase delay in the full bridges, the PV panels power is equally shared between the ports 2 and 3 of the TAFB. In other condition when a lagging phase delay is created in one of the ports (port 2) full bridge, complete power from the PV panels and also partial power from grid

network 2 (at port 3) is shared to grid network 2. From the active power graphs presented in section 4 it is validated that the TAFB circuit can be utilized for power diversion between the three ports as per the requirement. Also, the efficiency of the TAFB topology surpasses the efficiency of the conventional full bridge resonant converter proving effective performance of the proposed system.

REFERENCES

[1] Tze-Zhang Ang, Mohamed Salem, Mohamad Kamarol, Himadry Shekhar Das, Mohammad Alhuyi Nazari, Natarajan Prabaharan, "A comprehensive study of renewable energy sources: Classifications, challenges and suggestions," Energy Strategy Reviews,Volume 43,2022,100939,ISSN 2211-467X,https://doi.org/10.1016/j.esr.2022.100939.

[2] Kumar. J, C.R., Majid, M.A. Renewable energy for sustainable development in India: current status, future prospects, challenges, employment, and investment opportunities. *Energ Sustain Soc* **10**, 2 (2020). https://doi.org/10.1186/s13705-019-0232-1

[3] Poul Alberg Østergaard, Neven Duic, Younes Noorollahi, Soteris Kalogirou, "Advances in renewable energy for sustainable development," Renewable Energy,Volume 219, Part 1,2023,119377,ISSN 0960-1481,https://doi.org/10.1016/j.renene.2023.119377.

[4] Attou, Nasreddine & sid ahmed, Zidi & Khatir, Mohamed & Hadjeri, S.. (2020). Grid-Connected Photovoltaic System. 101-107. 10.1007/978-981-15-5444-5_13.

[5] A. Y. Mohammed, F. I. Mohammed and M. Y. Ibrahim, "Grid connected Photovoltaic system," *2017 International Conference on Communication, Control, Computing and Electronics Engineering (ICCCCEE)*, Khartoum, Sudan, 2017, pp. 1-5, doi: 10.1109/ICCCCEE.2017.7867659.

[6] Sotirios I. Nanou, Apostolos G. Papakonstantinou, Stavros A. Papathanassiou, "A generic model of two-stage grid-connected PV systems with primary frequency response and inertia emulation," Electric Power Systems Research,Volume 127,2015,Pages 186-196,ISSN 0378-7796,https://doi.org/10.1016/j.epsr.2015.06.011.

[7] Santoro, Danilo & Toscani, Andrea & Cova, Paolo & Delmonte, N.. (2024). "Triple active bridge converter in nanogrid applications: A direct interface for photovoltaic modules and storage." IET Power Electronics. 17. n/a-n/a. 10.1049/pel2.12674.

[8] H. Cao, L. Du, F. Guo, Z. Ma and Y. Zhao, "A Triple Active Bridge (TAB) Based Solid-State Transformer (SST) for DC Fast Charging Systems: Architecture and Control Strategy," *2023 IEEE Energy Conversion Congress and Exposition (ECCE)*, Nashville, TN, USA, 2023, pp. 855-860, doi: 10.1109/ECCE53617.2023.10362803.

[9] Pham, V.-L.; Wada, K. "Applications of Triple Active Bridge Converter for Future Grid and Integrated Energy Systems." *Energies* 2020, *13*, 1577. https://doi.org/10.3390/en13071577

[10] Wajahat Khan, Furkan Ahmad, Mohammad Saad Alam, "Fast EV charging station integration with grid ensuring optimal and quality power exchange," Engineering Science and Technology, an International Journal,Volume 22, Issue 1,2019,Pages 143-152,ISSN 2215-0986,https://doi.org/10.1016/j.jestch.2018.08.005.

[11] A. El Baset A. El Halim, Ahmed & Bayoumi, Ehab & El-Khattam, Walid & Ibrahim, Amr. (2023). Grid-Connected EV Fast Charging Stations Using Vector Control and CC-CV Techniques. 56. 993-1001. 10.18280/jesa.560610.

[12] S, Harini, Chellammal N, and Ramesh C Bansal. "Power Flow and Reliability Analysis of a Non-Isolated PV/Grid Connected Quasi Resonant Converter for off-Board EV Charging Station." *International Journal of Modelling and Simulation*, May, 1–16. 2024doi:10.1080/02286203.2024.2345239.

[13] Atawi, I.E.; Hendawi, E.; Zaid, S.A. Analysis and Design of a Standalone Electric Vehicle Charging Station Supplied by Photovoltaic Energy. *Processes* **2021**, *9*, 1246. https://doi.org/10.3390/pr9071246

[14] Q. Yan, B. Zhang and M. Kezunovic, "Optimized Operational Cost Reduction for an EV Charging Station Integrated With Battery Energy Storage and PV Generation," in *IEEE Transactions on Smart Grid*, vol. 10, no. 2, pp. 2096-2106, March 2019, doi: 10.1109/TSG.2017.2788440.

[15] Ratil H. Ashique, Zainal Salam, Mohd Junaidi Bin Abdul Aziz, Abdul Rauf Bhatti, “Integrated photovoltaic-grid dc fast charging system for electric vehicle: A review of the architecture and control,” Renewable and Sustainable Energy Reviews,Volume 69,2017,Pages 1243-1257,ISSN 1364-0321,https://doi.org/10.1016/j.rser.2016.11.245.

[16] Narasipuram, Rajanand & Mopidevi, Subbarao. “Parametric Modelling of Interleaved Resonant DC — DC Converter with Common Secondary Rectifier Circuit for xEV Charging Applications,” 2023, 842-846. 10.1109/ICSEIET58677.2023.10303318.

[17] Kılıçoğlu, Halise & Arya, Harshita & Das, Moumita & Tricoli, Pietro. (2022). “A New High-power Charging Points for Battery Electric Vehicles with Modular Push-pull Converters.” 581-586. 10.1109/SPEEDAM53979.2022.9842258.

[18] Rastgoo, S.; Mahdavi, Z.; Azimi Nasab, M.; Zand, M.; Padmanaban, S. Using an Intelligent Control Method for Electric Vehicle Charging in Microgrids. *World Electr. Veh. J.* **2022**, *13*, 222. https://doi.org/10.3390/wevj13120222

[19] S. Mukherjee and I. Sarkar, "A Brief Review on Triple Active Bridge DC-DC Converter," *2023 IEEE International Students' Conference on Electrical, Electronics and Computer Science (SCEECS)*, Bhopal, India, 2023, pp. 1-6, doi: 10.1109/SCEECS57921.2023.10063031.

[20] Z. Wang, Q. Luo, Y. Wei, D. Mou, X. Lu and P. Sun, "Topology Analysis and Review of Three-Port DC–DC Converters," in *IEEE Transactions on Power Electronics*, vol. 35, no. 11, pp. 11783-11800, Nov. 2020, doi: 10.1109/TPEL.2020.2985287.

[21] V. Nair R. *et al*., "Large Scale Grid Integration of Photovoltaic and Energy Storage Systems Using Triple Port Dual Active Bridge Converter Modules," *2018 IEEE Power & Energy Society General Meeting (PESGM)*, Portland, OR, USA, 2018, pp. 1-5, doi: 10.1109/PESGM.2018.8586158.

[22] Z. Wang and H. Li, "Integrated MPPT and bidirectional battery charger for PV application using one multiphase interleaved three-port dc-dc converter," *2011 Twenty-Sixth Annual IEEE Applied Power Electronics Conference and Exposition (APEC)*, Fort Worth, TX, USA, 2011, pp. 295-300, doi: 10.1109/APEC.2011.5744611.

[23] I. Askarian, M. Pahlevani and A. M. Knight, "Three-Port Bidirectional DC/DC Converter for DC Nanogrids," in *IEEE Transactions on Power Electronics*, vol. 36, no. 7, pp. 8000-8011, July 2021, doi: 10.1109/TPEL.2020.3046453.

[24] Y. Yu, K. Wada and Y. Kado, "Power Flow Control of DC Power Distribution Systems using Triple Active Bridge Converter in a Data Center," *2018 9th IEEE International Symposium on Power Electronics for Distributed Generation Systems (PEDG)*, Charlotte, NC, USA, 2018, pp. 1-6, doi: 10.1109/PEDG.2018.8447655.

[25] A. A. Ibrahim, A. Zilio, T. Younis, D. Biadene, T. Caldognetto and P. Mattavelli, "Optimal Modulation of Triple Active Bridge Converters by an Artificial-Neural- Network Approach," in *IEEE Transactions on Industrial Electronics*, vol. 71, no. 3, pp. 2590-2600, March 2024, doi: 10.1109/TIE.2023.3270529.